The reason for the importance placed on knowing the probability distribution for the different microstates is that once we have it, we can compute key observables such as the average current flowing through the channel or the average energy given by

$$\langle E \rangle = \sum_{i=1}^{N} E_i p(E_i), \tag{6.6}$$

where we have introduced the notation $\langle \cdots \rangle$ to indicate averages. What this equation tells us is that to find the average energy of the system, we sum over all of the energies of the possible microscopic outcomes, each weighted appropriately by its probability $p(E_i)$. One class of averages that will come to centerstage throughout the book is that concerned with the ligand occupancy, where we will compute the probability that a given receptor is bound as a function of the ligand concentration.

The Tricks Behind the Math: Differentiation with Respect to a Parameter The partition function serves as the analytical engine of statistical mechanics and permits us to directly calculate quantities such as the free energy ($G = -k_B T \ln Z$) and the average energy. To see the simple connection between the partition function and the average energy, we invoke a useful mathematical observation. Our interest is in the average energy, which can be written as

$$\langle E \rangle = \frac{1}{Z} \sum_{i=1}^{N} E_i e^{-E_i/k_B T}, \tag{6.7}$$

a result we obtain by substituting Equation 6.4 into Equation 6.6. Note that by virtue of the definition of the partition function as $Z = \sum_{i=1}^{N} e^{-E_i/k_B T}$, we can write the average energy as

$$\langle E \rangle = -\frac{1}{Z} \frac{\partial}{\partial \beta} Z, \tag{6.8}$$

where we have introduced the notation $\beta = 1/k_B T$. The point is that when we differentiate $e^{-\beta E_i}$ with respect to β, the result is $-E_i e^{-\beta E_i}$, exactly the quantity we need to compute the average. We can go even further by using the identity $d[\ln f(x)]/dx = (1/f)(df/dx)$. This permits us to rewrite Equation 6.8 as

$$\langle E \rangle = -\frac{\partial}{\partial \beta} \ln Z. \tag{6.9}$$

This very important trick will be used repeatedly for computing key observables of biological interest such as the probability that an ion channel is open and the average number of ligands bound to a receptor (such as the number of oxygen molecules bound to hemoglobin).

MATH

6.1.1 A First Look at Ligand–Receptor Binding

One of the most powerful uses to which we will put the tools developed in this chapter is to the broad class of binding interactions of interest in biology. Figure 6.1 introduced an example of the kinds of problems we will encounter and for which we can use the Boltzmann distribution and the partition function. Examples of this kind of

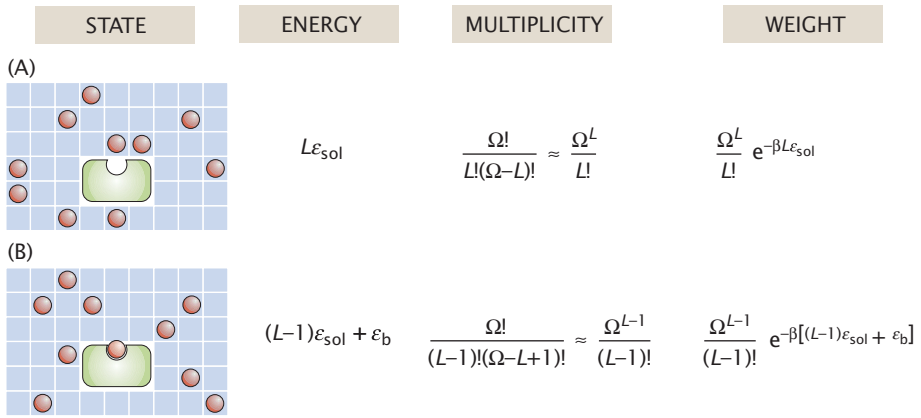

Figure 6.4: States and weights diagram for ligand–receptor binding. The cartoons show a lattice model of the solution for the case in which there are L ligands. In (A), the receptor is unoccupied. In (B), the receptor is occupied by a ligand and the remaining $L-1$ ligands are free in solution. A given state has a weight dictated by its Boltzmann factor. The multiplicity refers to the number of different microstates that share that same Boltzmann factor (for example, all of the states with no ligand bound to the receptor have the same Boltzmann factor).

binding include the binding of oxygen to hemoglobin, the binding of transcription factors to DNA, and the binding of acetylcholine to the nicotinic acetylcholine receptor. To examine the physics of Figure 6.1, imagine there are L ligand molecules in the box characterized by Ω lattice sites as well as a single receptor with one binding site as shown. For simplicity, we ignore any configurational degrees of freedom associated with the receptor itself. Our ambition is to compute the probability that a receptor is occupied by a ligand (p_{bound}) as a function of the number (or concentration) of ligands.

To see the logic of this calculation more clearly, Figure 6.4 shows the states available to this system, as well as their energies, their multiplicities, and overall statistical weights. The key point is that there are only two classes of states, namely, (i) all of those states for which there is no ligand bound to the receptor and (ii) all of those states for which one of the ligands is bound to the receptor. The neat feature of this situation is that although there are many realizations of each class of state, the Boltzmann factor is the same for each realization of these classes of state as shown in Figure 6.4.

To compute the probability that a ligand is bound, we need to construct a ratio in which the numerator is the weight of all states in which one ligand is bound to the receptor and the denominator is the sum over all states. This idea is represented graphically in Figure 6.5. What the figure shows is that there are a host of different states in which the receptor is occupied: first, there are L different ligands that can bind to the receptor; second, the $L-1$ ligands that remain behind in solution can be distributed amongst the Ω lattice sites in many different ways. In particular, we have

$$\text{weight when receptor occupied} = \underbrace{e^{-\beta\varepsilon_b}}_{\text{bound ligand}} \times \underbrace{\sum_{\text{solution}} e^{-\beta(L-1)\varepsilon_{sol}}}_{\text{free ligands}}, \tag{6.10}$$

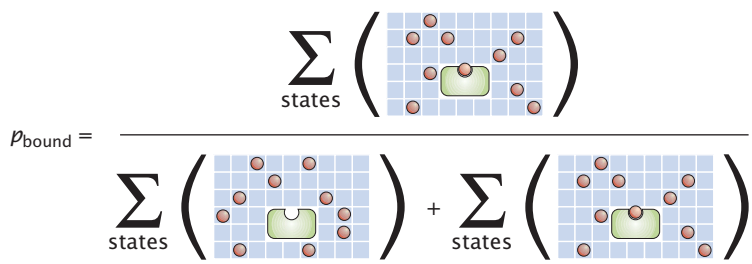

Figure 6.5: Probability of receptor occupancy. The figure shows how the probability of receptor occupancy can be written as a ratio of the weights of the favorable outcomes and the weights of *all* outcomes. The notation in the numerator instructs us to sum over the Boltzmann factors for all microstates of the system in which the receptor is occupied.

where we have introduced ε_b as the binding energy for the ligand and receptor and ε_{sol} as the energy for a ligand in solution. The summation $\sum_{solution}$ is an instruction to sum over all of the ways of arranging the $L-1$ ligands on the Ω lattice sites in solution, with each of those states assigned the weight $e^{-\beta(L-1)\varepsilon_{sol}}$. Since the Boltzmann factor is the same for each of these states, what this sum amounts to is finding the number of arrangements of the $L-1$ ligands amongst the Ω lattice sites, which yields

$$\sum_{\text{solution}} e^{-\beta(L-1)\varepsilon_{sol}} = \frac{\Omega!}{(L-1)![\Omega-(L-1)]!} e^{-\beta(L-1)\varepsilon_{sol}}. \tag{6.11}$$

The denominator of the expression shown in Figure 6.5 is the partition function itself, since it represents the sum over *all* possible arrangements of the system (both those with the receptor occupied and not) and is given by

$$Z(L,\Omega) = \underbrace{\sum_{\text{solution}} e^{-\beta L\varepsilon_{sol}}}_{\text{none bound}} + \underbrace{e^{-\beta\varepsilon_b} \sum_{\text{solution}} e^{-\beta(L-1)\varepsilon_{sol}}}_{\text{ligand bound}}. \tag{6.12}$$

We have already evaluated the second term in the sum culminating in Equation 6.11. To complete our evaluation of the partition function, we have to evaluate the sum $\sum_{solution} e^{-\beta L\varepsilon_{sol}}$ over all of the ways of arranging the L ligands on the Ω lattice sites, with the result

$$\sum_{\text{solution}} e^{-\beta L\varepsilon_{sol}} = e^{-\beta L\varepsilon_{sol}} \frac{\Omega!}{L!(\Omega-L)!}. \tag{6.13}$$

In light of these results, the partition function can be written as

$$Z(L,\Omega) = e^{-\beta L\varepsilon_{sol}} \frac{\Omega!}{L!(\Omega-L)!} + e^{-\beta\varepsilon_b} e^{-\beta(L-1)\varepsilon_{sol}} \frac{\Omega!}{(L-1)![\Omega-(L-1)]!}. \tag{6.14}$$

We can now simplify this result by using the approximation that

$$\frac{\Omega!}{(\Omega-L)!} \approx \Omega^L, \tag{6.15}$$

which is justified as long as $\Omega \gg L$. The approximation amounts to taking the largest term in the sum that would result from resolving the parentheses in Equation 6.15. To see why this is a good approximation, consider the case when $\Omega = 10^6$ and $L = 10$, resulting in

$$\frac{10^6!}{(10^6-10)!} = 10^6 \times (10^6-1) \times (10^6-2) \times \cdots \times (10^6-9) \approx (10^6)^{10}. \tag{6.16}$$

The error made by effecting this approximation can be seen by multiplying out all the terms in parentheses in Equation 6.16 and keeping the terms of order $(10^6)^9$. We find that this next term has the value $45 \times (10^6)^9$, which is roughly four orders of magnitude smaller than the leading term, demonstrating the legitimacy of the approximation.

With these results in hand, we can now write p_{bound} as

$$p_{bound} = \frac{e^{-\beta\varepsilon_b} \frac{\Omega^{L-1}}{(L-1)!} e^{-\beta(L-1)\varepsilon_{sol}}}{\frac{\Omega^L}{L!} e^{-\beta L\varepsilon_{sol}} + e^{-\beta\varepsilon_b} \frac{\Omega^{L-1}}{(L-1)!} e^{-\beta(L-1)\varepsilon_{sol}}}. \tag{6.17}$$

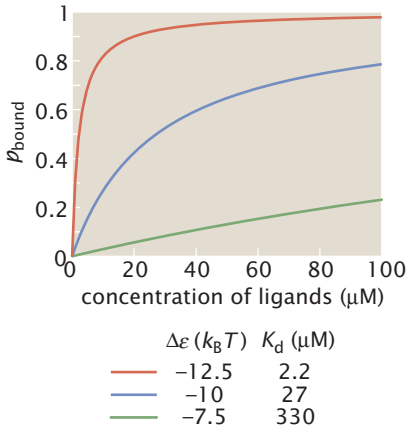

Figure 6.6: Average occupancy as a function of ligand concentration. The figure shows the average number of ligands bound as a function of the number of ligands in solution. The plot shows curves for three choices of $\Delta\varepsilon$: -7.5, -10, and -12.5 k_BT, and a standard state $c_0 = 0.6$ M. The binding energies are also translated into the language of equilibrium dissociation constants.

This result can be simplified by multiplying the top and bottom by $(L!/\Omega^L)e^{\beta L\varepsilon_{sol}}$, resulting in

$$p_{bound} = \frac{(L/\Omega)e^{-\beta\Delta\varepsilon}}{1 + (L/\Omega)e^{-\beta\Delta\varepsilon}}, \tag{6.18}$$

where we have defined $\Delta\varepsilon = \varepsilon_b - \varepsilon_{sol}$. The overall volume of the box is V_{box} and this permits us to rewrite our results using concentration variables. In particular, this can be written in terms of ligand concentration $c = L/(\Omega V_{box})$, where ΩV_{box} is the total volume considered. We introduce $c_0 = 1/V_{box}$, a "reference" concentration (effectively, an arbitrary "standard state") corresponding to having all sites in the lattice occupied. This results in

$$p_{bound} = \frac{(c/c_0)e^{-\beta\Delta\varepsilon}}{1 + (c/c_0)e^{-\beta\Delta\varepsilon}}. \tag{6.19}$$

This classic result goes under many different names depending upon the field (such as the Langmuir adsorption isotherm or a Hill function with Hill coefficient $n = 1$). Regardless of names, this expression will be our point of departure for thinking about all binding problems. Though many problems of biological interest exhibit binding curves that are "sharper" than this one (that is, they exhibit cooperativity—to be discussed in detail in Chapter 7), ultimately, even those curves are measured against the standard result derived here.

To make a simple estimate of the parameters appearing in Equation 6.19, we choose the size of the elementary boxes in our lattice model to be 1 nm^3, which corresponds to $c_0 \approx 0.6$ M. This is comparable to the standard state of 1 M used in many biochemistry textbooks. Given this choice of standard state, we can plot p_{bound} as a function of the concentration of ligands for different choices of the binding energy with characteristic binding energies ranging from -7.5 to -12.5 k_BT. The result is plotted in Figure 6.6. As said before, many problems in statistical mechanics can be seen as the playing out of a competition between energetic and entropic contributions to the overall free energy. In this case, the interesting concentration of ligand corresponds to that choice of L for which the two terms in the denominator of Equation 6.17 are approximately equal. Equality of these two terms roughly amounts to the statement that the entropy lost in stealing one of the ligands from solution to bind it to the receptor is just made up for by the energetic gain ($\Delta\varepsilon$) associated with binding the ligand to the receptor. Notice also that this concentration corresponds to having half occupancy ($p_{bound} = 0.5$). At low concentrations, the entropic term is dominant, while at high enough concentrations, the energetic term dominates.

6.1.2 The Statistical Mechanics of Gene Expression: RNA Polymerase and the Promoter

An exciting application of the ideas on ligand–receptor binding developed above is to the problem of gene regulation. Cells make "decisions" all the time. One of the key manifestations of cellular decision making is the expression of different genes at different places at different times and to different extents. In Section 3.2.1, we introduced the central dogma. However, our treatment of replication, transcription, and translation was barren because it failed to acknowledge all of the possible cellular interventions that can occur during each of these processes. Figure 6.7 shows a more complete view of the processes

which tells us that the probability of a given state is proportional to the Gibbs factor (that is, $p(E_s^{(1)}, N_s^{(1)}) \propto e^{-(E_s^{(1)} - \mu N_s^{(1)})/k_B T}$). As a result, the probability of finding the system in state i with energy $E_s^{(i)}$ and particle number $N_s^{(i)}$ is

$$p(E_s^{(i)}, N_s^{(i)}) = \frac{e^{-\beta(E_s^{(i)} - \mu N_s^{(i)})}}{\mathcal{Z}}, \tag{7.15}$$

a result known as the Gibbs distribution, where we have defined the grand partition function as

$$\mathcal{Z} = \sum_i e^{-\beta(E_s^{(i)} - N_s^{(i)}\mu)}. \tag{7.16}$$

This equation instructs us to sum over all of the possible microstates (labeled by i).

In Section 6.1, we argued that the partition function serves as the analytical engine of statistical mechanics and illustrated that claim by showing how the average energy $\langle E \rangle$ can be computed as a derivative of the partition function (see Equation 6.9 on p. 241). The grand partition function permits us to go further and to compute the average number of particles in our system as

$$\langle N \rangle = \frac{1}{\beta} \frac{\partial}{\partial \mu} \ln \mathcal{Z}. \tag{7.17}$$

To see this, we note that the average particle number can be written as

$$\langle N \rangle = \frac{1}{\mathcal{Z}} \sum_i N_i e^{-\beta(E_i - N_i \mu)}, \tag{7.18}$$

where we have dropped the cumbersome notation involving subscript "s" to signify that we are referring to the "system." Indeed, from now on, whenever we invoke the Gibbs distribution, we will tacitly assume that the terms E_i and N_i refer exclusively to our system, which is in contact with a hybrid thermal–particle reservoir. What this perspective offers from the point of view of our microscopic models is that the chemical potential serves as a shorthand for the explicit treatment of the reservoir.

7.2.2 Simple Ligand–Receptor Binding Revisited

To apply the Gibbs distribution, we revisit the problem of ligand–receptor binding introduced in Sections 6.1.1 (p. 241) and 6.4.1 (p. 270). In this case, we imagine a slightly different setup where all of our attention is focused on a single receptor that is in contact with the surrounding heat bath and particle reservoir. The beauty of treating the problem in this way is that it will provide a much simpler treatment of the particles in the reservoir than was offered by the Boltzmann distribution. Further, this approach will permit us to generalize easily to more complicated cases such as hemoglobin in which there are multiple binding sites. In this case, the receptor can be in one of two states, bound or unbound, with σ serving as an indicator of the state of binding, with $\sigma = 0$ corresponding to the unbound state and $\sigma = 1$ to the bound state. The energy in this case is $E = \varepsilon_b \sigma$, where $\varepsilon_b < 0$, revealing a favorable interaction between ligand and receptor. The particular choices of σ are arbitrary and had we made different choices, then we would have had to make a corresponding change in

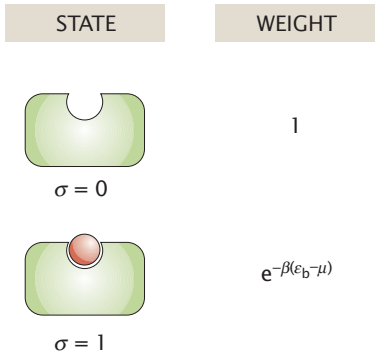

Figure 7.10: States and weights for ligand–receptor binding. The schematic shows the states of the receptor and their corresponding statistical weights as computed using the Gibbs distribution.

the energy. The virtue of this particular choice of the σ's is that $\langle\sigma\rangle$ reports the average number of bound ligands. The states and weights for our ligand–receptor problem are shown in Figure 7.10.

Using the grand canonical distribution as the basis of our evaluation of $\langle N\rangle$, we need to evaluate

$$\mathcal{Z} = \sum_{\text{states}} e^{-\beta(E_{\text{state}} - N_{\text{state}}\mu)}, \tag{7.19}$$

where we have switched notation to sum over "states" instead of the nondescript index i. The variable $\beta = 1/k_B T$ reflects the contact of the system with a thermal reservoir and the presence of μ reflects contact with a particle reservoir. The sum over states is very simple since there are only two states to consider, namely, (i) the state where the receptor is not occupied, which is characterized by $\sigma = 0$, and (ii) the state where the receptor is occupied, which is characterized by $\sigma = 1$. As a result, we write

$$\mathcal{Z} = \sum_{\sigma=0}^{1} e^{-\beta(\varepsilon_b \sigma - \mu\sigma)}. \tag{7.20}$$

The resulting sum is of the form

$$\mathcal{Z} = 1 + e^{-\beta(\varepsilon_b - \mu)}. \tag{7.21}$$

The average number of ligands bound is equal to the normalized weight of the occupied state, and is given by

$$\langle N\rangle = \frac{e^{-\beta(\varepsilon_b - \mu)}}{1 + e^{-\beta(\varepsilon_b - \mu)}}. \tag{7.22}$$

This result can also be computed by taking the derivative as described in Equation 7.17.

For the case of a receptor that can bind only one ligand, the average number of bound ligands, $\langle N\rangle$, is equivalent to the quantity p_{bound} introduced in Chapter 6. As a result, the calculation done here should yield precisely the same result we found in Equation 6.19 (p. 244). To see that equivalence, we recall that the chemical potential of an ideal solution can be written as $\mu = \mu_0 + k_B T \ln(c/c_0)$ as shown in Section 6.2.2 (p. 262). If we substitute this expression for the chemical potential into Equation 7.22, we find

$$\langle N\rangle = \frac{(c/c_0)e^{-\beta\Delta\varepsilon}}{1 + (c/c_0)e^{-\beta\Delta\varepsilon}}, \tag{7.23}$$

where we have introduced the notation $\Delta\varepsilon = \varepsilon_b - \mu_0$. Here $\Delta\varepsilon$ is the energy difference upon taking the ligand from solution and placing it on the receptor. This result is equivalent to that found in Chapter 6. We have revisited the problem of ligand–receptor binding for two reasons. First, the present treatment gives us a chance to see the idea of our internal state variables σ in action. Second, this example also served as our maiden example of the use of the Gibbs distribution which will be used again to describe O_2 binding in hemoglobin, the equilibrium accessibility of nucleosomes, and other problems as well.

7.2.3 Phosphorylation as an Example of Two Internal State Variables

The idea of a two-state system is extremely powerful in biology and applies to many cases beyond those already mentioned. One

amino acid can also be rapidly dephosphorylated by a protein phosphatase enzyme, the signal can be just as quickly switched off, and then switched back on again if need be, without the need to degrade or resynthesize the transcription factor. Interestingly, for most two-component systems, the phosphatase activity is carried out by the same sensor histidine kinase protein that was responsible for the phosphorylation in the first place.

7.2.4 Hemoglobin as a Case Study in Cooperativity

In Section 4.2 (p. 143), we argued that hemoglobin has served as the classic example of ligand–receptor binding. One of the rich features offered by hemoglobin above and beyond the results for simple ligand–receptor binding we have already obtained in Sections 6.1.1 (p. 241), 6.4.1 (p. 270), and 7.2.2 is the existence of cooperativity. Cooperativity refers to the fact that the binding energy for a given ligand depends upon the number of ligands that are already bound to the receptor. Intuitively, the cooperativity idea results from the fact that when a ligand binds to a protein, it will induce some conformational change. As a result, when the next ligand binds, it finds an altered protein interface and hence experiences a different binding energy (characterized by a different equilibrium constant). This effect is reflected in binding data as shown in Figure 4.4 (p. 144). From the point of view of statistical mechanics, we will interpret cooperativity as an interaction energy—that is, the energies of the various ligand binding reactions are not simply additive.

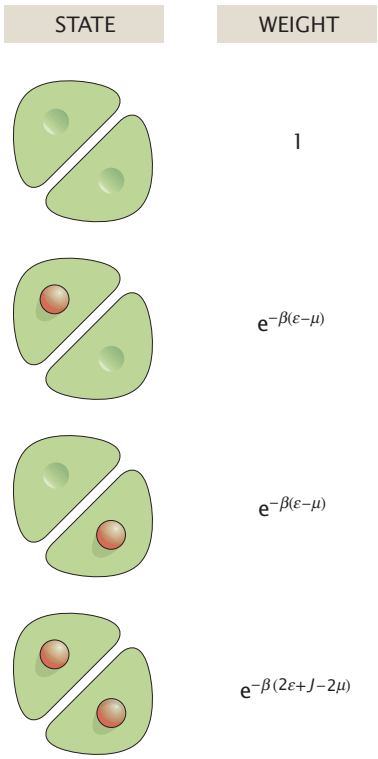

Figure 7.17: States and weights diagram for a toy model of dimoglobin. Each state of occupancy is characterized by a pair (σ_1, σ_2) denoting whether the first and second sites are occupied by an oxygen molecule. The weights show the Gibbs factors for each of the different states.

The Binding Affinity of Oxygen for Hemoglobin Depends upon Whether or Not Other Oxygens Are Already Bound

In keeping with the overarching theme of the chapter, our treatment of ligand–receptor binding in the classic case of hemoglobin can be couched in the language of two-state occupation variables. In particular, for hemoglobin, we describe the state of the system with the vector $(\sigma_1, \sigma_2, \sigma_3, \sigma_4)$, where σ_i takes the values 0 (unbound) or 1 (bound) characterizing the occupancy of site i within the molecule. Figure 4.6 (p. 146) showed the structure of hemoglobin revealing the four binding sites for oxygen molecules. One of the main goals of a model like this is to address questions such as the average number of bound oxygen molecules as a function of the oxygen concentration (or partial pressure).

A Toy Model of a Dimeric Hemoglobin (Dimoglobin) Illustrate the Idea of Cooperativity

In order to make analytic progress in revealing the precise nature of cooperativity, we examine a toy model that reflects some of the full complexity of binding in hemoglobin. In particular, we imagine a fictitious dimoglobin molecule that has two O_2-binding sites. (Indeed, some clams actually do have a dimeric hemoglobin instead of a tetrameric hemoglobin like most other animals.) We begin by identifying the states and weights as shown in Figure 7.17. This molecule is characterized by four distinct states corresponding to each of the binding sites of the dimoglobin molecule being either occupied or empty. For example, if binding site 1 is occupied then we have $\sigma_1 = 1$,

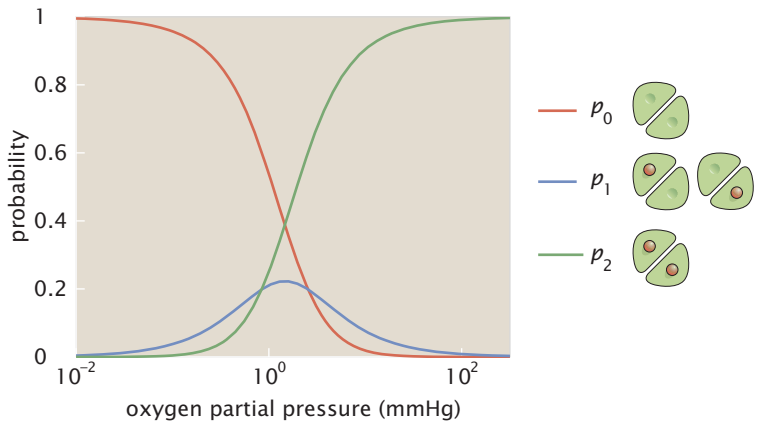

Figure 7.18: Probabilities of oxygen binding to dimoglobin. The plot shows the probability of finding no oxygen molecules bound to dimoglobin (p_0), that of finding one molecule bound (p_1), and that of finding two molecules bound (p_2). The parameters used are $\Delta\varepsilon = -5\ k_B T$, $J = -2.5\ k_B T$, and $c_0 = 760$ mmHg.

and if it is unoccupied then $\sigma_1 = 0$. The energy of the system can be written as

$$E = \varepsilon(\sigma_1 + \sigma_2) + J\sigma_1\sigma_2, \tag{7.29}$$

where ε is the energy associated with an oxygen being bound to one of the two sites. The parameter J is a measure of the cooperativity and implies that when both sites are occupied, the energy is not just the sum of the individual binding energies.

The grand partition function is obtained by summing over the four states shown in Figure 7.17 and is given by

$$\mathcal{Z} = \underbrace{1}_{\text{unoccupied}} + \underbrace{e^{-\beta(\varepsilon-\mu)} + e^{-\beta(\varepsilon-\mu)}}_{\text{single occupancy}} + \underbrace{e^{-\beta(2\varepsilon+J-2\mu)}}_{\text{both sites occupied}}. \tag{7.30}$$

With the partition function in hand, we can compute the probabilities of each of the distinct classes of states: unoccupied, single occupancy, double occupancy. In Figure 7.18, we plot these probabilities as a function of the oxygen partial pressure.

Using Equation 7.17, we can find the average occupancy as a function of the ligand chemical potential as

$$\langle N \rangle = \frac{2e^{-\beta(\varepsilon-\mu)} + 2e^{-\beta(2\varepsilon+J-2\mu)}}{1 + e^{-\beta(\varepsilon-\mu)} + e^{-\beta(\varepsilon-\mu)} + e^{-\beta(2\varepsilon+J-2\mu)}}. \tag{7.31}$$

This simple result now permits us to write the occupancy in terms of the concentration of oxygen by remembering that $\mu = \mu_0 + k_B T \ln(c/c_0)$ (this was shown in Section 6.2.2 on p. 262), and it is given by

$$\langle N \rangle = \frac{2(c/c_0)e^{-\beta\Delta\varepsilon} + 2(c/c_0)^2 e^{-\beta(2\Delta\varepsilon+J)}}{1 + 2(c/c_0)e^{-\beta\Delta\varepsilon} + (c/c_0)^2 e^{-\beta(2\Delta\varepsilon+J)}}, \tag{7.32}$$

where we define $\Delta\varepsilon = \varepsilon - \mu_0$. This result is shown in Figure 7.19. To further probe the nature of cooperativity, a useful exercise is to examine the occupancy in the case where the interaction term J is zero. In this case, we find the average occupancy is given by the sum of two independent single-site occupancies as

$$\langle N \rangle = 2\frac{(c/c_0)e^{-\beta\Delta\varepsilon}}{1 + (c/c_0)e^{-\beta\Delta\varepsilon}}. \tag{7.33}$$

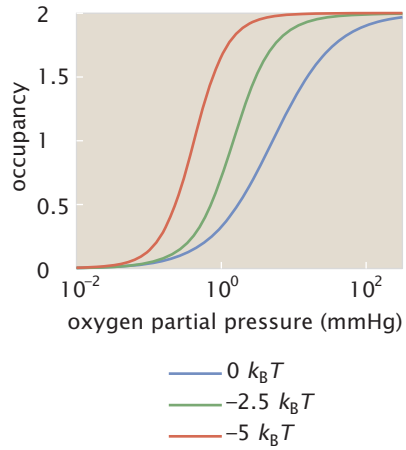

Figure 7.19: Average number of oxygen molecules bound to dimoglobin as a function of oxygen concentration. The parameters used to make the plots are $\Delta\varepsilon = \varepsilon_b - \mu_0 = -5\ k_B T$, $c_0 = 760$ mmHg and $J = 0$ (no cooperativity), $J = -2.5\ k_B T$ and $J = -5\ k_B T$.

The Monod–Wyman–Changeux (MWC) Model Provides a Simple Example of Cooperative Binding

One of the classic two-state models for binding is the Monod–Wyman–Changeux (MWC) model for cooperative binding. The essence of the model is that the protein of interest can exist in two distinct conformational states known as "tense" (T) and "relaxed" (R). In the absence of ligand, the T state of the protein is favored over the R state. We represent this unfavorable energy cost to access the R state with the energy ε. However, the interesting twist is that the ligand-binding reaction has a higher affinity for the R state. This has the effect that with increasing ligand concentration, the balance will be tipped toward the R state, despite the cost, ε, of accessing that state. We label the binding energies ε_T and ε_R, which signify the favorable energy upon binding to the molecule when it is in the T and R states, respectively. If we maintain our use of σ_1 and σ_2 to characterize the state of ligand occupancy of our toy model of dimoglobin and, in addition, introduce the variable σ_m to indicate whether the molecule is in the T ($\sigma_m = 0$) or R ($\sigma_m = 1$) state, then the energy of our system can be written as

$$E = (1 - \sigma_m)\varepsilon_T \sum_{i=1}^{2} \sigma_i + \sigma_m \left(\varepsilon + \varepsilon_R \sum_{i=1}^{2} \sigma_i \right). \tag{7.34}$$

In order to find the occupancy (that is, $\langle N \rangle$) of the dimoglobin, we need to compute the grand partition function. As usual, it is illuminating to depict the various allowed states and their corresponding statistical weights as shown in Figure 7.20. There are a total of eight distinct states and we can sum over all of them to obtain the grand partition function

$$\mathcal{Z} = \underbrace{1 + 2e^{-\beta(\varepsilon_T - \mu)} + e^{-\beta(2\varepsilon_T - 2\mu)}}_{\text{T terms}} + \underbrace{e^{-\beta\varepsilon}(1 + 2e^{-\beta(\varepsilon_R - \mu)} + e^{-\beta(2\varepsilon_R - 2\mu)})}_{\text{R terms}}. \tag{7.35}$$

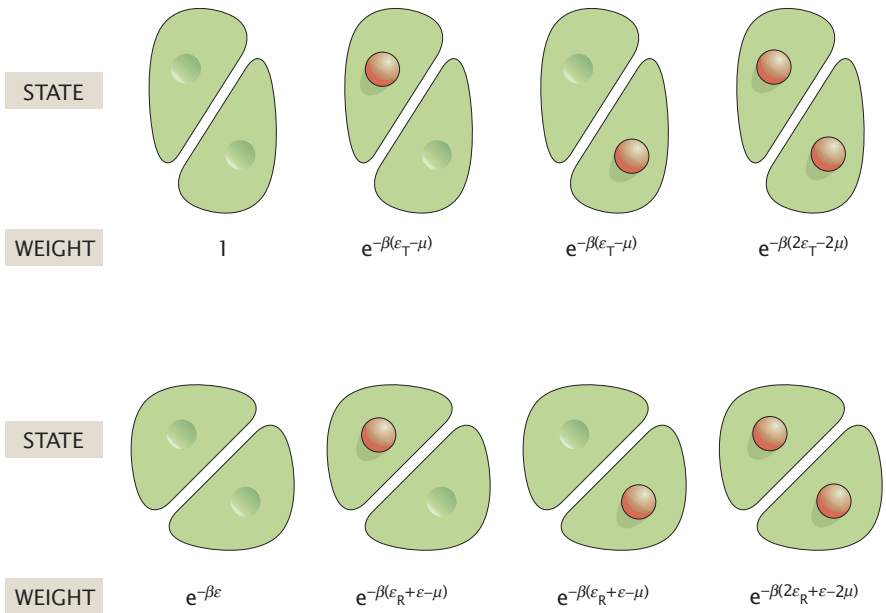

Figure 7.20: States and weights for the MWC model. The upper row shows the occupancies for the T state of the molecule and the lower row shows the occupancies for the R state of the molecule. The set of allowed states amounts to permitting 0, 1, or 2 O_2 molecules to bind to either the T or the R state of the molecule.

As usual, we can find the average occupancy by evaluating

$$\langle N \rangle = k_B T \frac{\partial}{\partial \mu} (\ln \mathcal{Z}),$$

with the result

$$\langle N \rangle = \frac{2}{\mathcal{Z}} [x + x^2 + e^{-\beta\varepsilon}(y + y^2)], \tag{7.36}$$

where we have defined $x = (c/c_0)e^{-\beta(\varepsilon_T - \mu_0)}$ and $y = (c/c_0)e^{-\beta(\varepsilon_R - \mu_0)}$. The average number of bound ligands as a function of the concentration of oxygen is shown in Figure 7.21.

Using the hypothetical molecule dimoglobin, we have examined oxygen binding from several different perspectives. The first model we introduced is mechanistically more detailed. On the other hand, in many practical cases involving real proteins the coupling energies cannot be easily measured. In such circumstances, the MWC approximation allows quantitative treatments of cooperative protein behavior using only two states and a few parameters. This can be particularly useful when there are many different ligands interacting with the same protein, each of which can affect its overall enzymatic activity.

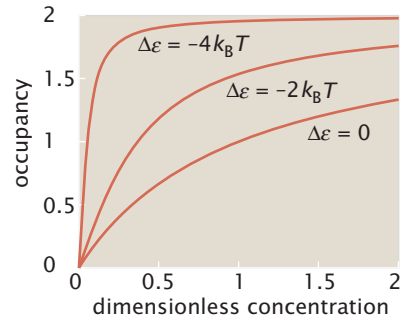

Figure 7.21: Average number of bound receptors in dimoglobin for the MWC model. The dimensionless concentration is written as $x = (c/c_0)e^{-\beta(\varepsilon_T - \mu_0)}$, where ε_T is the binding free energy of the ligand in the tense state. $\Delta\varepsilon$ is the difference between the binding energy in the relaxed and tense states. For the plots shown here, $\varepsilon = 2\, k_B T$.

Statistical Models of the Occupancy of Hemoglobin Can Be Written Using Occupation Variables

Using the simple occupation variable formalism introduced above, we can now examine a hierarchy of models that have been set forth in the attempt to understand cooperative oxygen binding in hemoglobin. In each of these cases, the occupation variable language permits a simple statement of the degree of oxygen binding. Further, the energy of the system itself both with and without cooperativity may be easily written in this language. In particular, we now characterize the binding state of the hemoglobin molecule with four state variables, $\{\sigma_1, \sigma_2, \sigma_3, \sigma_4\}$. Each of these variables can take the value 0 or 1, with $\sigma_\alpha = 0$ corresponding to site α unoccupied and $\sigma_\alpha = 1$ corresponding to site α occupied by an oxygen. Figure 7.22 shows a series of models of hemoglobin binding that account for the cooperativity with different degrees of sophistication.

There is a Logical Progression of Increasingly Complex Binding Models for Hemoglobin

Noncooperative Model We begin with the simplest model, in which the binding on the different sites is independent. In this case, the energy of the system is given by

$$E = \varepsilon \sum_{\alpha=1}^{4} \sigma_\alpha, \tag{7.37}$$

where ε is the energy associated with an oxygen molecule binding to one of the sites on hemoglobin. As usual, the injunction of statistical mechanics is to use the energy in order to compute the partition function. In this case, the grand partition function corresponds to summing over the 16 possible states of the system corresponding to all of the choices of the σ_i. More concretely, the grand partition function is written as

$$\mathcal{Z} = \sum_{\sigma_1=0}^{1} \sum_{\sigma_2=0}^{1} \sum_{\sigma_3=0}^{1} \sum_{\sigma_4=0}^{1} e^{-\beta(\varepsilon - \mu)\sum_{\alpha=1}^{4} \sigma_\alpha}. \tag{7.38}$$

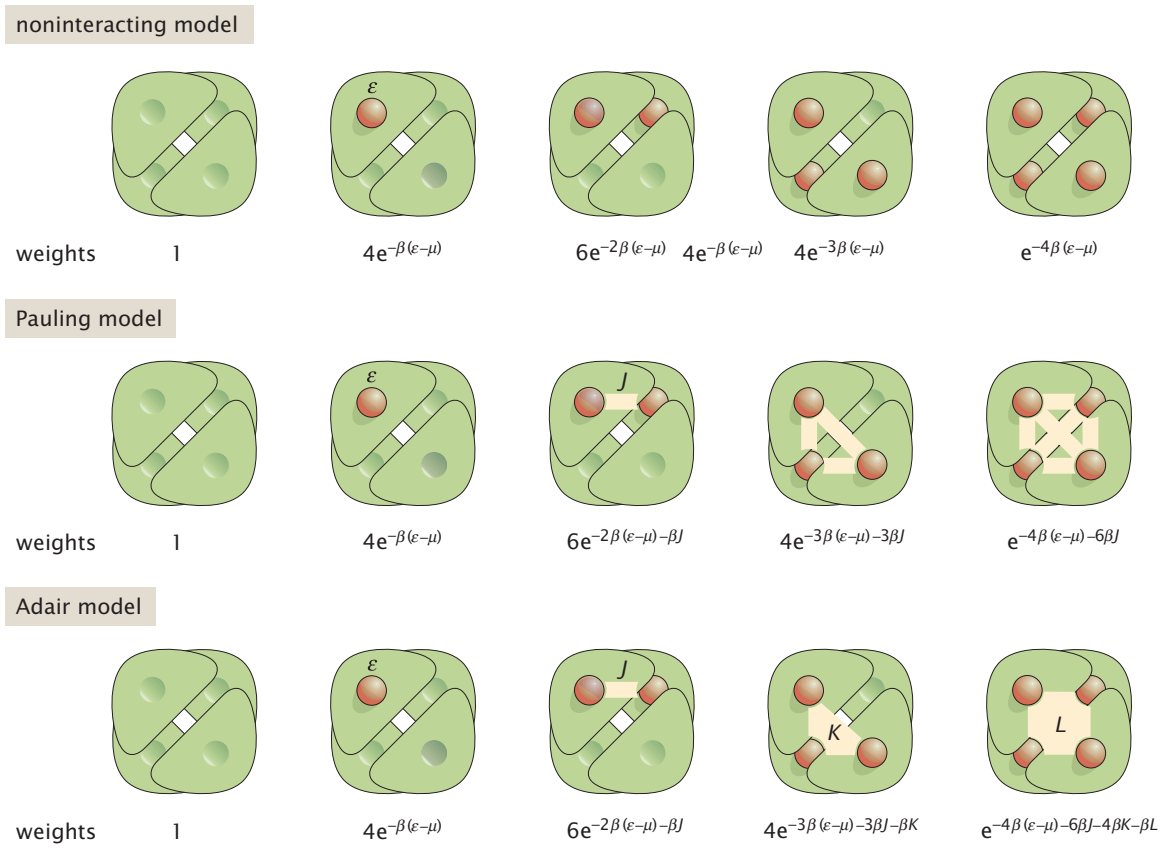

Figure 7.22: Hierarchy of models that can be used to characterize the cooperativity in oxygen binding to hemoglobin. In each case, four state variables $\{\sigma_1, \sigma_2, \sigma_3, \sigma_4\}$ are used to characterize whether the four sites are occupied by oxygen or not. The difference from one model to the next is how the energy depends upon the four state variables. These differences are reflected in the statistical weights for the different states.

By noting that each of the terms is independent, this may be simplified to the form

$$\mathcal{Z} = \sum_{\sigma_1=0}^{1} e^{-\beta(\varepsilon-\mu)\sigma_1} \sum_{\sigma_2=0}^{1} e^{-\beta(\varepsilon-\mu)\sigma_2} \sum_{\sigma_3=0}^{1} e^{-\beta(\varepsilon-\mu)\sigma_3} \sum_{\sigma_4=0}^{1} e^{-\beta(\varepsilon-\mu)\sigma_4}. \quad (7.39)$$

These sums are each evaluated to $1 + e^{-\beta(\varepsilon-\mu)}$ and, as a result, the total partition function is of the form

$$\mathcal{Z} = (1 + e^{-\beta(\varepsilon-\mu)})^4. \quad (7.40)$$

To find the occupancy of a given hemoglobin molecule, we resort to the usual trick introduced in Equation 7.17. For the result given in Equation 7.40, this yields

$$\langle N \rangle = \frac{4e^{-\beta(\varepsilon-\mu)}}{1 + e^{-\beta(\varepsilon-\mu)}}. \quad (7.41)$$

We can rewrite this result in terms of the oxygen concentration by using our simple model of the chemical potential, namely, $\mu = \mu_0 + k_B T \ln(c/c_0)$, with the result that the occupancy is given by

$$\langle N \rangle = 4 \frac{(c/c_0)e^{-\beta(\varepsilon-\mu_0)}}{1 + (c/c_0)e^{-\beta(\varepsilon-\mu_0)}}. \quad (7.42)$$

Note that this result is just four times the result we would obtain for a single binding site—ligand binding to the different sites is completely independent. If we compare this model with observed oxygen binding curves as shown in Figure 7.23, we see that the noncooperative binding model is completely inconsistent with the data.

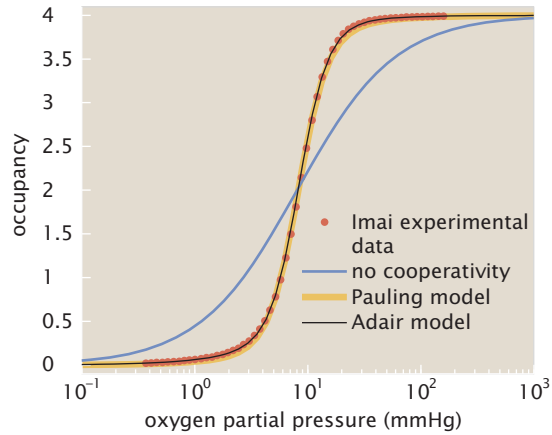

Figure 7.23: Hemoglobin binding. Comparison of the oxygen binding isotherms for different models of hemoglobin using the two-level system description. (Data from K. Imai, *Biophys. Chem.* 37:1, 1990.)

Pauling Model The next model in this hierarchy of models that can be written in the language of the two-state system is the so-called Pauling model. In this case, there is no change to the way in which we characterize the system using the set of variables $\{\sigma_1, \sigma_2, \sigma_3, \sigma_4\}$. What changes from one example to the next is our choice of energy function. In the case of the Pauling model, the physical content of the cooperativity arises because it is assumed that there is a pairwise interaction between oxygens on different sites. If we think of the four binding sites as the vertices of a tetrahedron, there are six interactions corresponding to the six edges of the tetrahedron. If we label the four vertices $1, 2, 3$, and 4, these pairwise interactions are between 1 and 2, 1 and 3, etc. and there are a total of six distinct such interactions.

Within this model, the energy of the system is written in the form

$$E = \varepsilon \sum_{\alpha=1}^{4} \sigma_\alpha + \frac{J}{2} \sum_{(\alpha,\gamma)}{}' \sigma_\alpha \sigma_\gamma, \tag{7.43}$$

where the sums over α and γ run from 1 to 4, the prime $\sum'$ instructs us *not* to include terms in the sum when $\alpha = \gamma$, and J is divided by 2 to account for the presence of terms like $\sigma_1\sigma_2$ and $\sigma_2\sigma_1$ which both occur in the sum. Whenever two different sites are occupied, there is a corresponding term in the energy with a contribution J. The partition function corresponding to this energy is given by

$$\mathcal{Z} = \sum_{\sigma_1=0}^{1} \sum_{\sigma_2=0}^{1} \sum_{\sigma_3=0}^{1} \sum_{\sigma_4=0}^{1} e^{-\beta(\varepsilon-\mu)\sum_{\alpha=1}^{4}\sigma_\alpha - \beta(J/2)\sum_{\alpha,\gamma}{}'\sigma_\alpha\sigma_\gamma}, \tag{7.44}$$

which once again corresponds to summing over all 16 states of occupancy of the hemoglobin molecule by its partner oxygens. As before, the partition function can be evaluated analytically and is given by

$$\mathcal{Z} = \underbrace{1}_{\text{0 bound}} + \underbrace{4e^{-\beta(\varepsilon-\mu)}}_{\text{1 bound}} + \underbrace{6e^{-2\beta(\varepsilon-\mu)-\beta J}}_{\text{2 bound}} + \underbrace{4e^{-3\beta(\varepsilon-\mu)-3\beta J}}_{\text{3 bound}} + \underbrace{e^{-4\beta(\varepsilon-\mu)-6\beta J}}_{\text{4 bound}}. \tag{7.45}$$

Once the partition function is in hand, computing the average occupancy is a matter of computing a single derivative of the form given in Equation 7.17, resulting in

$$\langle N \rangle = \frac{4e^{-\beta(\varepsilon-\mu)} + 12e^{-\beta(\varepsilon-\mu)-\beta J} + 12e^{-3\beta(\varepsilon-\mu)-3\beta J} + 4e^{-4\beta(\varepsilon-\mu)-6\beta J}}{1 + 4e^{-\beta(\varepsilon-\mu)} + 6e^{-2\beta(\varepsilon-\mu)-\beta J} + 4e^{-3\beta(\varepsilon-\mu)-3\beta J} + e^{-4\beta(\varepsilon-\mu)-6\beta J}}. \tag{7.46}$$

If we adopt the notation $j = e^{-\beta J}$ and $x = (c/c_0)e^{-\beta(\varepsilon-\mu_0)}$, then we are left with

$$\langle N \rangle = \frac{4x + 12x^2 j + 12x^3 j^3 + 4x^4 j^6}{1 + 4x + 6x^2 j + 4x^3 j^3 + x^4 j^6}. \tag{7.47}$$

The beauty of this model is that it is entirely minimalistic and involves only two free parameters. Further, this model reduces to the noncooperative model for a particular choice of parameters. In particular, if $J = 0$ (that is, $j = 1$), this abolishes the cooperativity and we restore our earlier result of Equation 7.42. In the problems at the end of the chapter, the reader is invited to examine the data in Figure 7.23 using this model.

Adair Model The next level in the hierarchy of models that we examine is the so-called Adair model, which goes beyond the Pauling model in accounting for three- and four-body interactions. What this means concretely is that if three sites are occupied by oxygens, there is an energy that is different than the sum of all of the pair interactions. The reason for the proliferation of parameters (four parameters in the Adair model, in comparison with two in the Pauling model) is to account for the richness of the binding data, which can include competitive binding by other ligands and mutants of the hemoglobin protein. The reader is referred back to Figure 7.22 to get a sense for the types of interactions included in the Adair model. The energy in the Adair model is written as

$$E = \varepsilon \sum_{\alpha=1}^{4} \sigma_\alpha + \frac{J}{2} {\sum_{\alpha,\gamma}}' \sigma_\alpha \sigma_\gamma + \frac{K}{3!} {\sum_{\alpha,\beta,\gamma}}' \sigma_\alpha \sigma_\beta \sigma_\gamma + \frac{L}{4!} {\sum_{\alpha,\beta,\gamma,\delta}}' \sigma_\alpha \sigma_\beta \sigma_\gamma \sigma_\delta, \tag{7.48}$$

where the parameters K and L capture the energy of the three- and four-body interactions, respectively. Note that the sums for the terms involving the parameters K and L are only over those cases where the σ's refer to different binding sites as indicated by the prime on the summation sign.

The grand partition function for this model has the same basic structure as we found in the previous cases. In particular, we are invited to sum over the 16 distinct binding configurations of the molecule, with each one assigned the appropriate energy. This results in the somewhat daunting expression

$$\mathcal{Z} = \sum_{\sigma_1=0}^{1} \sum_{\sigma_2=0}^{1} \sum_{\sigma_3=0}^{1} \sum_{\sigma_4=0}^{1} \exp\left[-\beta(\varepsilon - \mu) \sum_{\alpha=1}^{4} \sigma_\alpha - \frac{J}{2} {\sum_{\alpha,\beta}}' \sigma_\alpha \sigma_\beta - \frac{K}{3!} {\sum_{\alpha,\beta,\gamma}}' \sigma_\alpha \sigma_\beta \sigma_\gamma - \frac{L}{4!} {\sum_{\alpha,\beta,\gamma,\delta}}' \sigma_\alpha \sigma_\beta \sigma_\gamma \sigma_\delta \right]. \tag{7.49}$$

On the other hand, this expression is not nearly as bad as it looks, and the partition function can be evaluated, resulting in

$$\mathcal{Z} = \underbrace{1}_{\text{0 bound}} + \underbrace{4e^{-\beta(\varepsilon-\mu)}}_{\text{1 bound}} + \underbrace{6e^{-2\beta(\varepsilon-\mu)-\beta J}}_{\text{2 bound}} + \underbrace{4e^{-3\beta(\varepsilon-\mu)-3\beta J-\beta K}}_{\text{3 bound}} + \underbrace{e^{-4\beta(\varepsilon-\mu)-6\beta J-4\beta K-\beta L}}_{\text{4 bound}}. \tag{7.50}$$

As before, the occupancy is obtained by evaluating the derivative with respect to the chemical potential using Equation 7.17, and this

results in

$$\langle N\rangle = \frac{4x + 12x^2 j + 12x^3 j^3 k + 4x^4 j^6 k^4 l}{1 + 4x + 6x^2 j + 4x^3 j^3 k + x^4 j^6 k^4 l}, \tag{7.51}$$

where we have introduced the notation $k = e^{-\beta K}$ and $l = e^{-\beta L}$. In the absence of the interaction terms (that is, $j = k = l = 1$), we once again recover the result in Equation 7.42.

Another way of viewing the results of this section is shown in Figure 7.24. These plots illustrate the probability of the various allowed states of the system as a function of the concentration of oxygen. In particular, we plot the probability of finding no oxygen bound (p_0), one oxygen bound (p_1), and so on. By comparing Figures 7.24(A) and (B), we see that in the case of cooperative binding, the intermediate states are effectively eliminated, with the dominant states being either unoccupied or saturated. The reader is invited to examine this result in more detail in the problems at the end of the chapter.

We have considered a hierarchy of models for the binding of oxygen in hemoglobin. As shown in the analysis, all of these models can be written in terms of the two-state occupation variables $\{\sigma_i\}$ and their differences correspond to the different ways in which they handle cooperativity (which we conveniently model as interactions between the different binding sites). One of the key outputs of these models is the binding curves, which show how the occupancy depends upon the concentration of oxygen. We compare these different models in Figure 7.23, where it is seen that the Pauling and Adair models have introduced cooperativity. The parameters we use to obtain these curves come from measurements on the equilibrium constants for hemoglobin binding in which the binding curves are *fit* to the functional form

$$\langle N\rangle = \frac{4K_1 x + 12K_1K_2x^2 + 12K_1K_2K_3x^3 + 4K_1K_2K_3K_4x^4}{1 + 4K_1 x + 6K_1K_2x^2 + 4K_1K_2K_3x^3 + K_1K_2K_3K_4x^4}, \tag{7.52}$$

with the parameters $K_1 = 1.51 \times 10^{-2}\,\text{mmHg}^{-1}$, $K_2 = 1.52 \times 10^{-2}\,\text{mmHg}^{-1}$, $K_3 = 3.47 \times 10^{-1}\,\text{mmHg}^{-1}$, and $K_4 = 3.2\,\text{mmHg}^{-1}$. "Cooperativity" is one of the key facts of biochemical interaction.

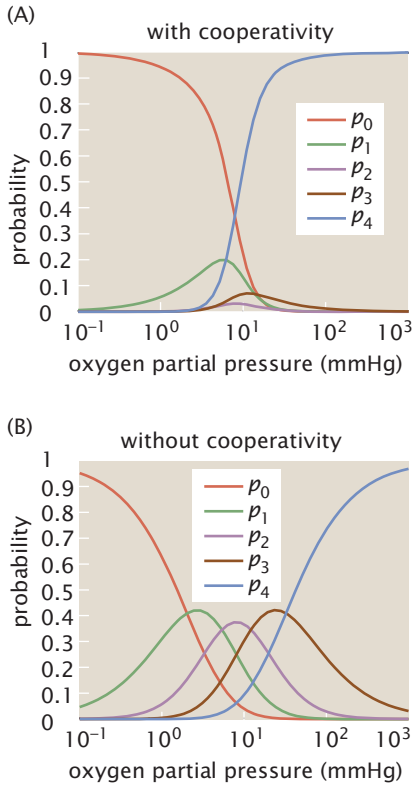

Figure 7.24: Probability of various states in hemoglobin binding. The plot shows the probabilities of the states p_0, p_1, p_2, p_3, and p_4, where p_n refers to the probability of the state with n oxygen molecules bound to the hemoglobin. (A) Adair model treatment of the probabilities of the different states (parameters shown after Equation 7.52). (B) Plot for the case in which there is no cooperativity in the model ($K_d = 8.07\,\text{mmHg}$).

7.3 Ion Channels Revisited: Ligand-Gated Channels and the MWC Model

Earlier in the chapter, we began our discussion of two-state systems by appealing to the example of ion channels. We noted that there are many different kinds of driving forces that can tip the balance between the closed and open states. Ligand-gated channels are ion channels whose opening and closing is regulated by binding of ligands to the protein that makes up the channel. One of the best studied examples is the nicotinic acetylcholine receptor, which plays a role in the neuromuscular junction. It has two binding sites for acetylcholine and the equilibrium between the open and closed state of the channel is shifted toward the open state by the binding of acetylcholine, as shown in Figure 7.25.

To study the opening of the channel as a function of acetylcholine concentration we make use of a statistical mechanics model of a channel, which is analogous to the Monod–Wyman–Changeux (MWC) model of dimoglobin discussed in Section 7.2.4. In the dimoglobin case, the protein was in the T or R state and the ligand had a higher affinity for